Multi-wavelength observations to understand the solar magnetic activity and its feedback on the interplanetary medium

G. Molodij, B.Schmieder and V. Bommier

LESIA-Observatoire de Paris-Meudon, CNRS, associé à l'Université Pierre et Marie Curie-Paris 06 et à l'Université Diderot-Paris 07.

Courtesy of Dr. G. Aulanier

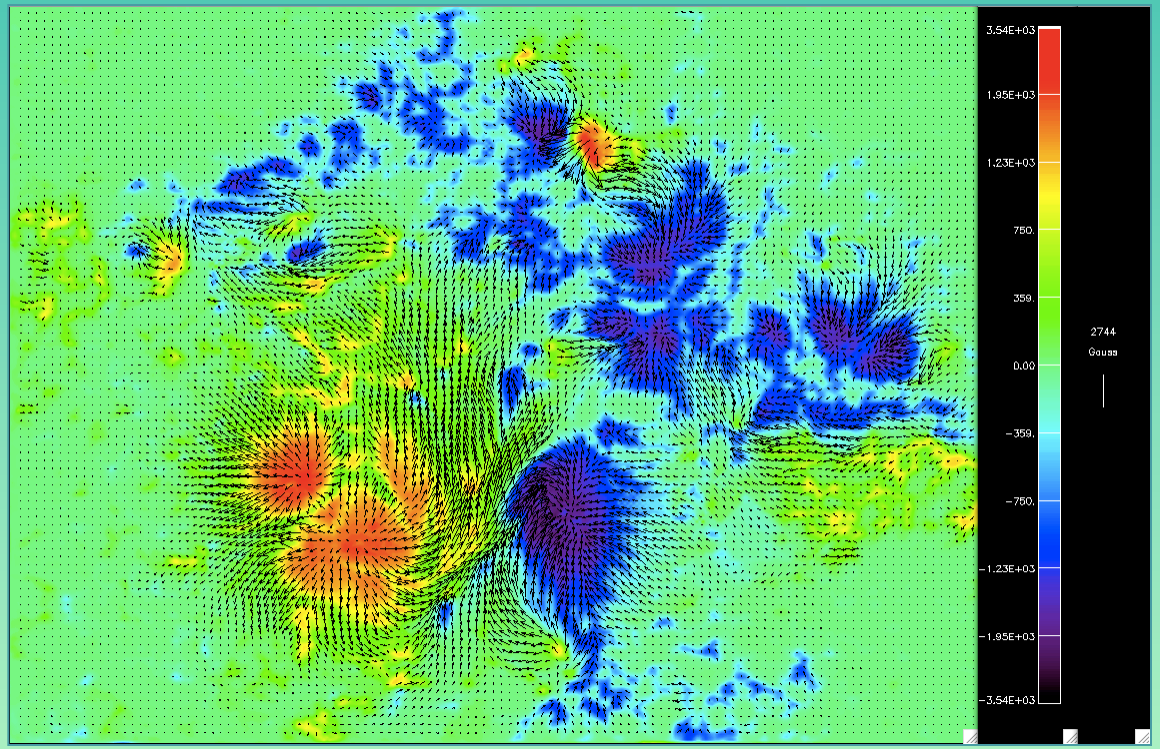

Transient phenomena in the Sun-Earth system

21-23 November, 2003

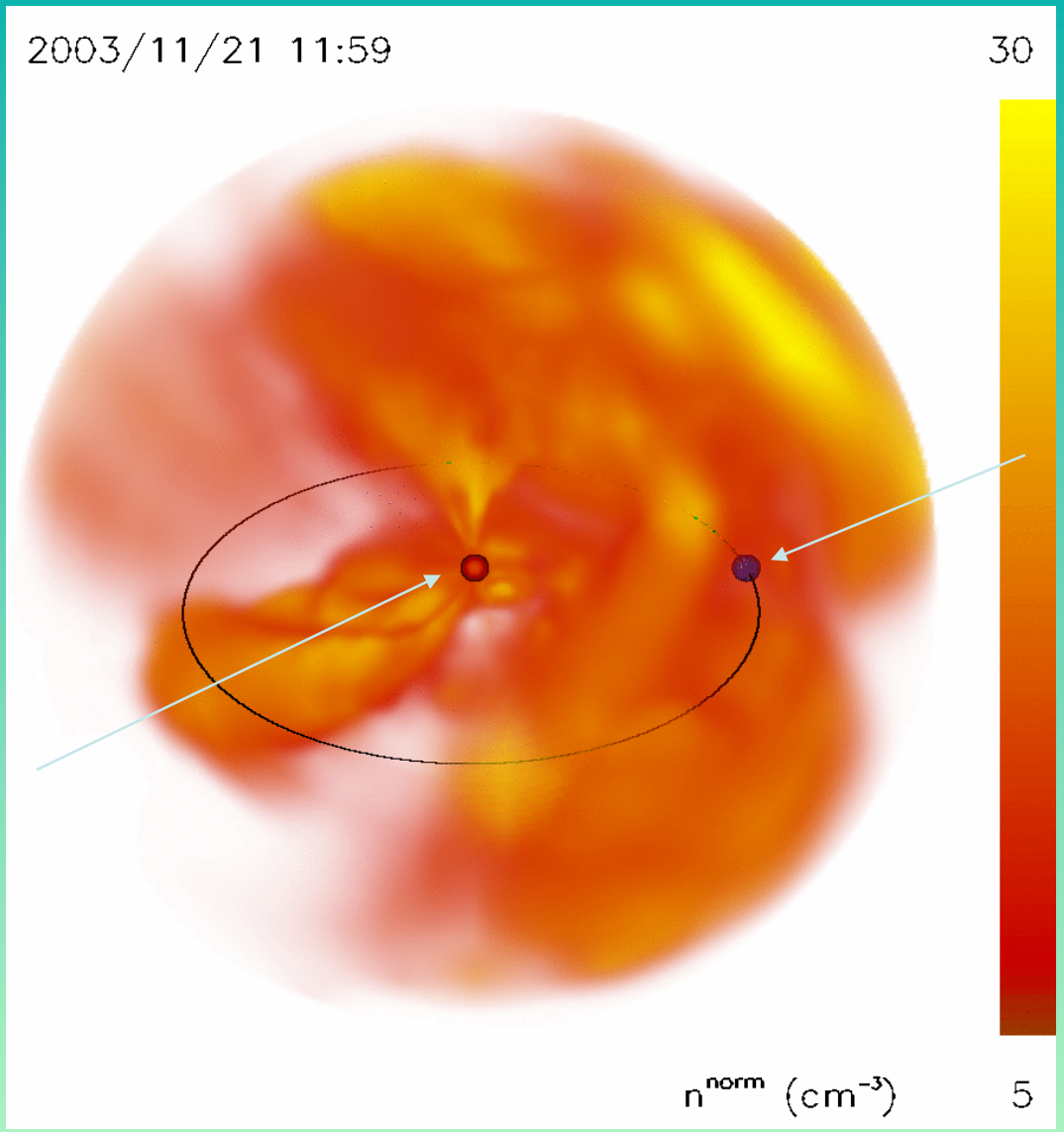

Earth

Sun

Courtesy of
Dr P. Manohoran

Interplanetary magnetic cloud (Ooty scintillation measurements)

Interplanetar Coronal Mass Ejection arriving at the Earth

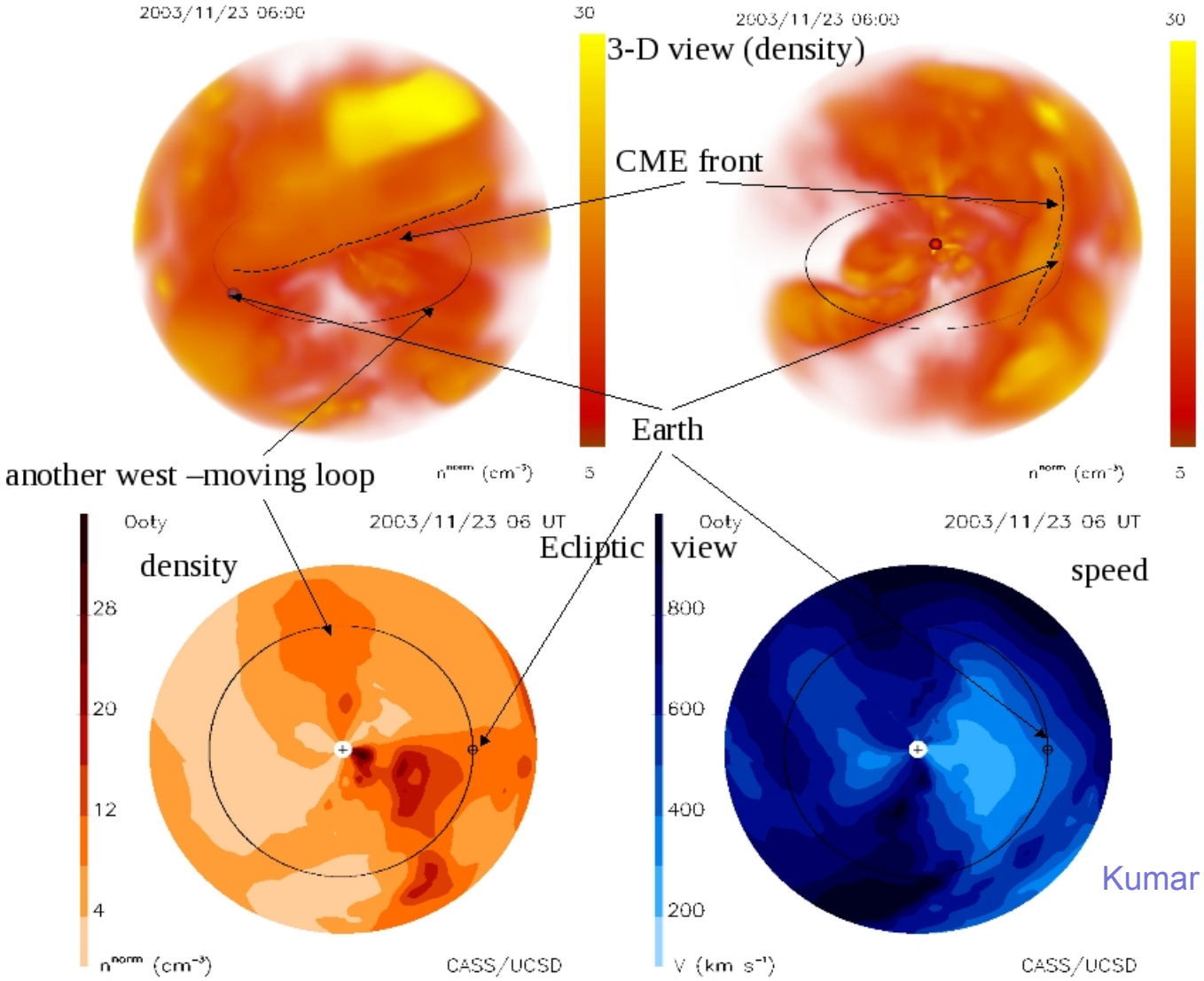

Kumar et al 2009

Ooty IPS images show the flux rope orientation of 70 deg w.r.t Ecliptic plane

Associate solar events and magnetic clouds

Magnetogram MDI (photosphere)

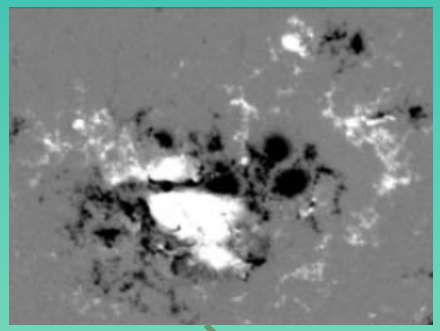

Hα (chromosphere) Nainital

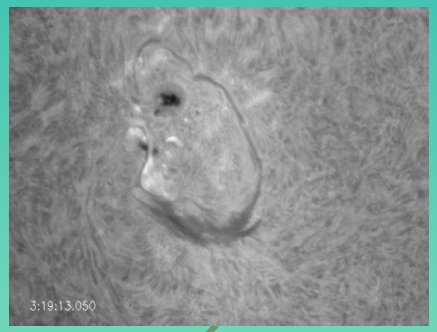

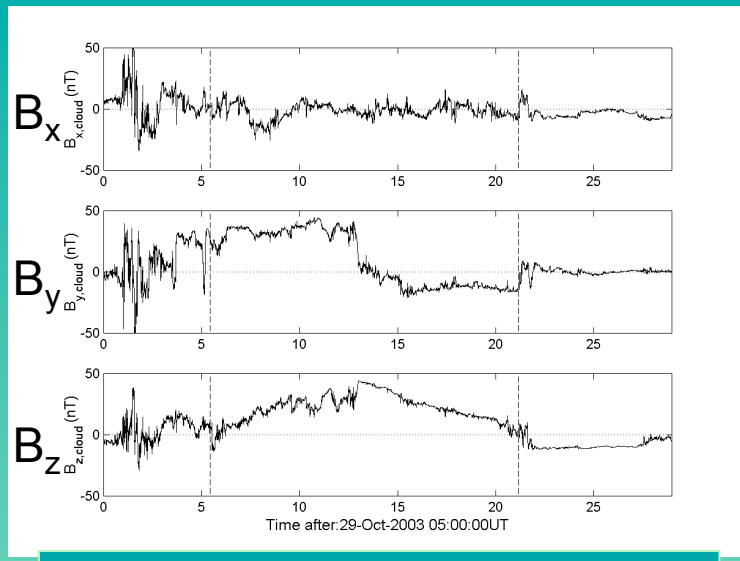

In Situ (Advanced Composition Explorer)

ACE

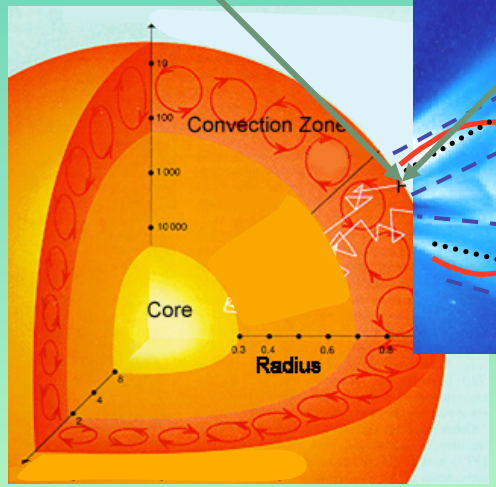

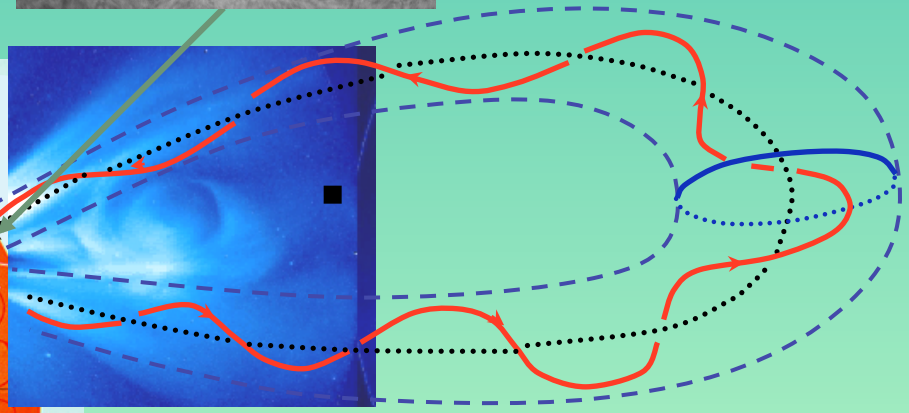

Ejection CME

Associate solar events and magnetic clouds

Scintillation (detection of interstellar coronal mass ejection)

Multiwavelength observations

- Solar events: remote measurements
- CME velocity, timing (1-5 days)
- Localization of active region
- Measure in situ of magnetic clouds

Magnetism (orientation, flux helicity)

- Topology
- Magnetic field extrapolation

Solar events on 18 November (LASCO)

Flare 2
Partial halo CME
v ~1220 km/s

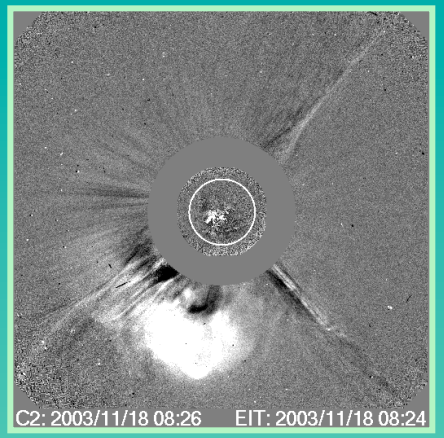

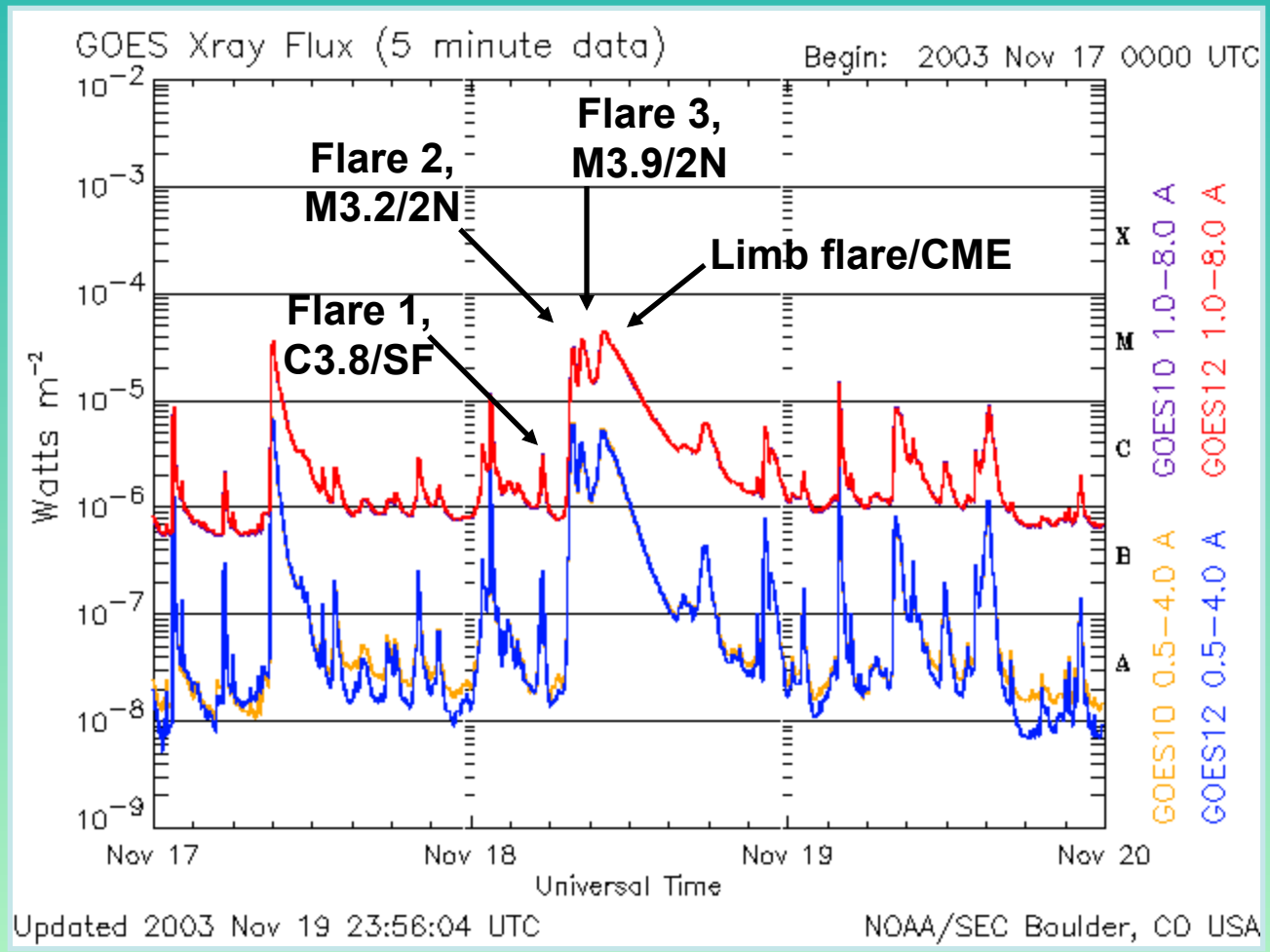

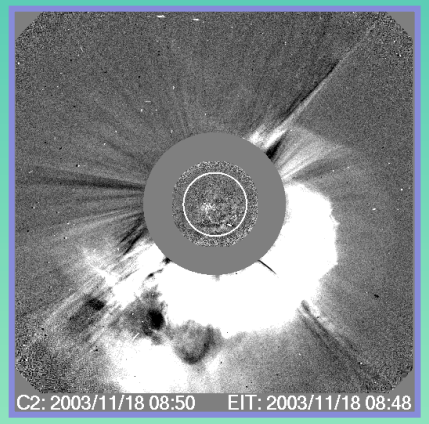

Flare 3
Full halo CME,
v ~1660 km/s

Solar events identification on 20 November

CME associated with Flares

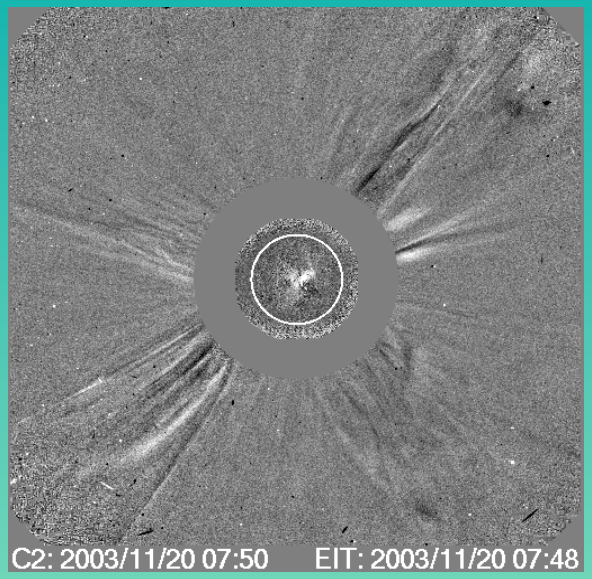

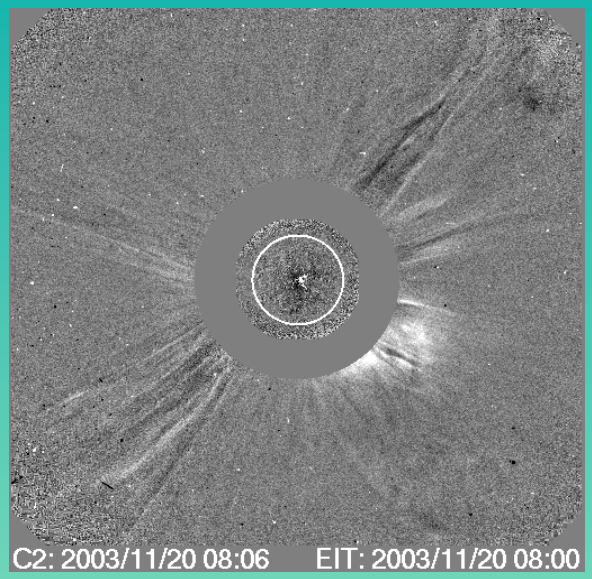

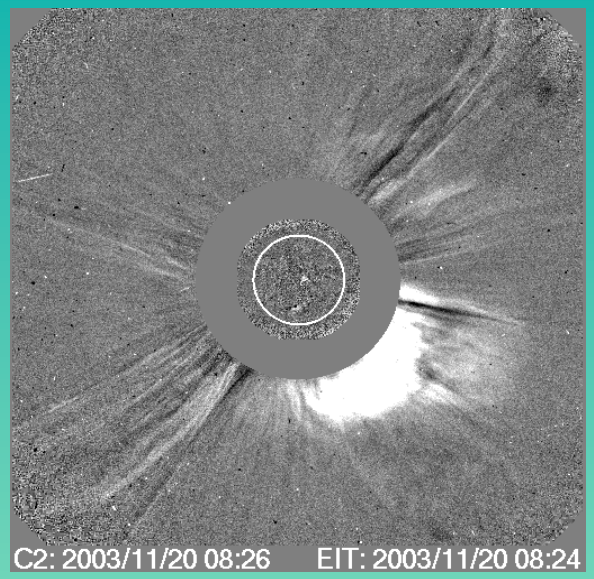

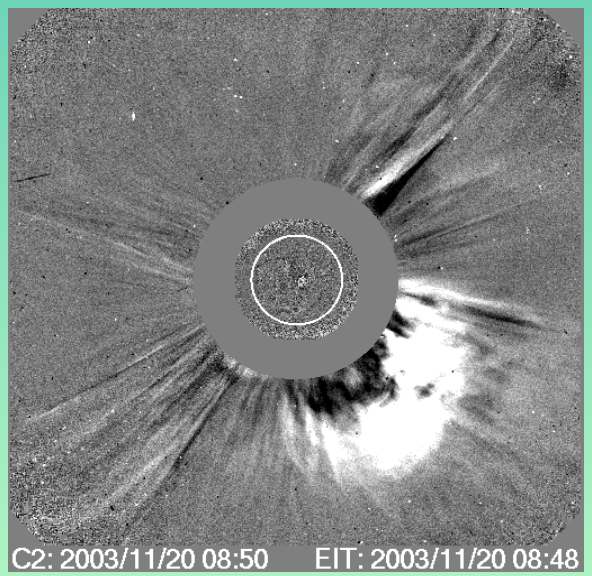

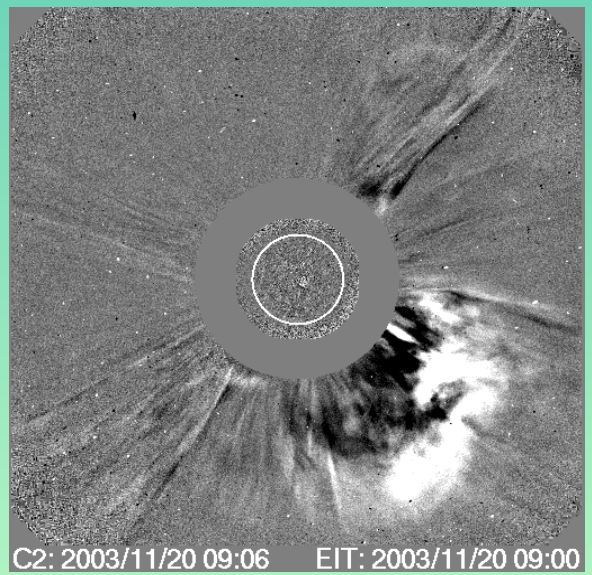

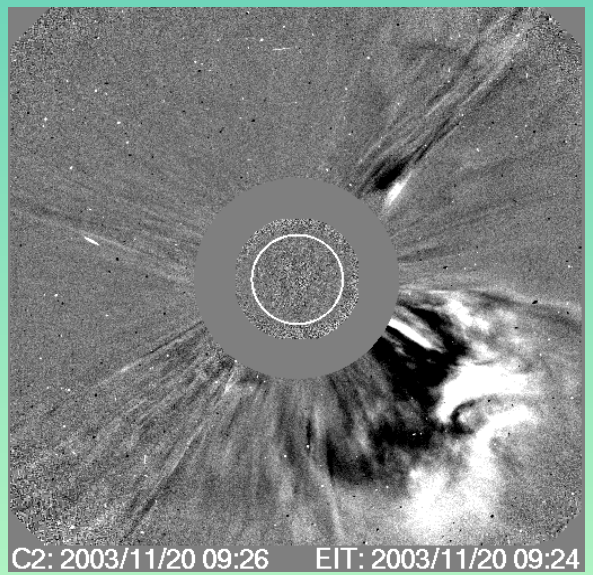

Most geoeffective case of solar cycle 23: Dst=-472 nT

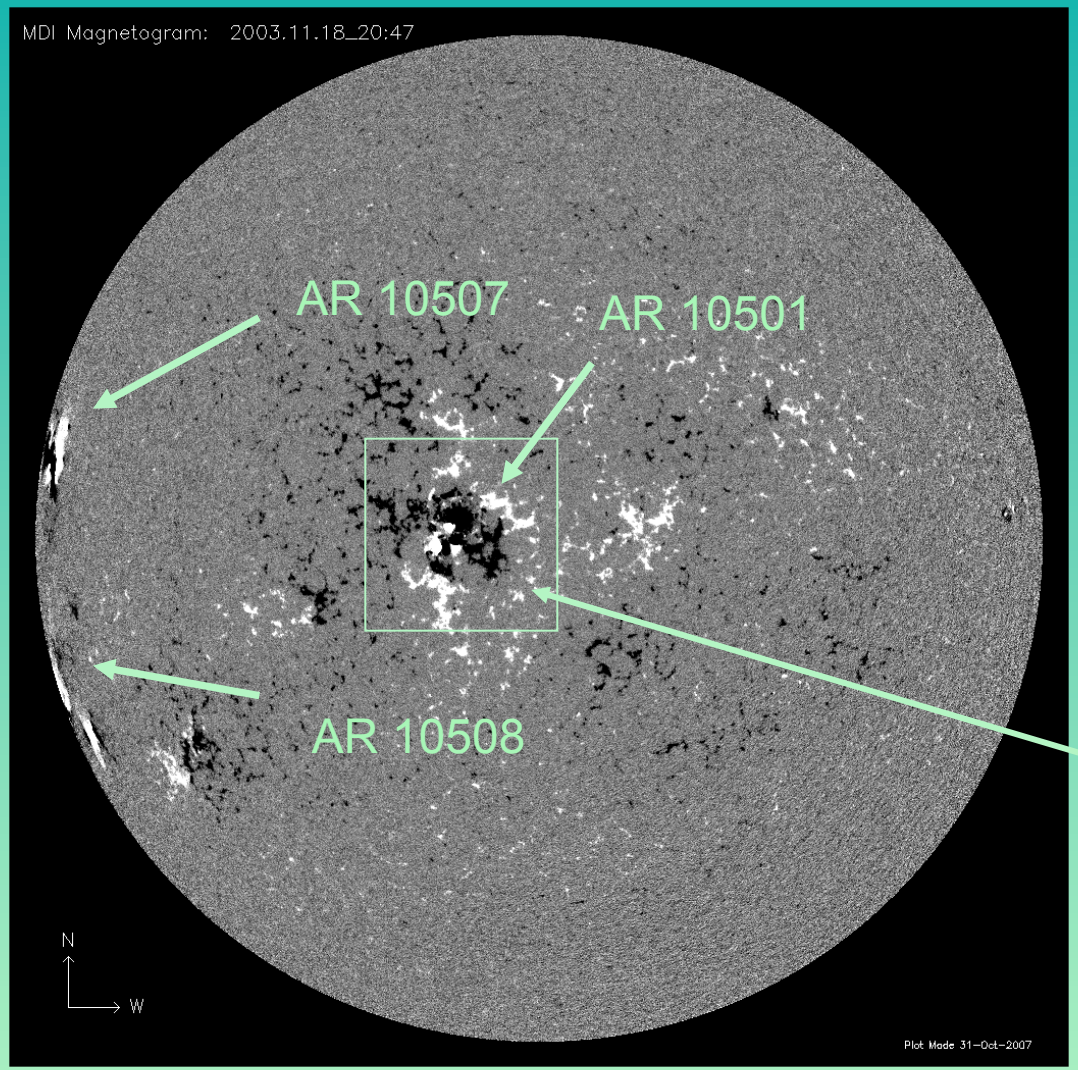

Magnetic field 18 November 2003

AR 10501, 10507 and 10508 were the return of:

AR 10484, 10488 and 10486 (Halloween events)

The magnetic storm is associated with a magnetic cloud on November 20 and this AR

Gopalswamy et al. (2005), Yurchyshyn et al. (2005), Möstl et al. (2008), Chandra et al. (2010), Schmieder et al (2010, 2011)

Observational clues – Active region helicity sign

Sunspot whorls ⇒ $H_{AR} < 0$

ARIES image

Observational clues – Active region helicity sign

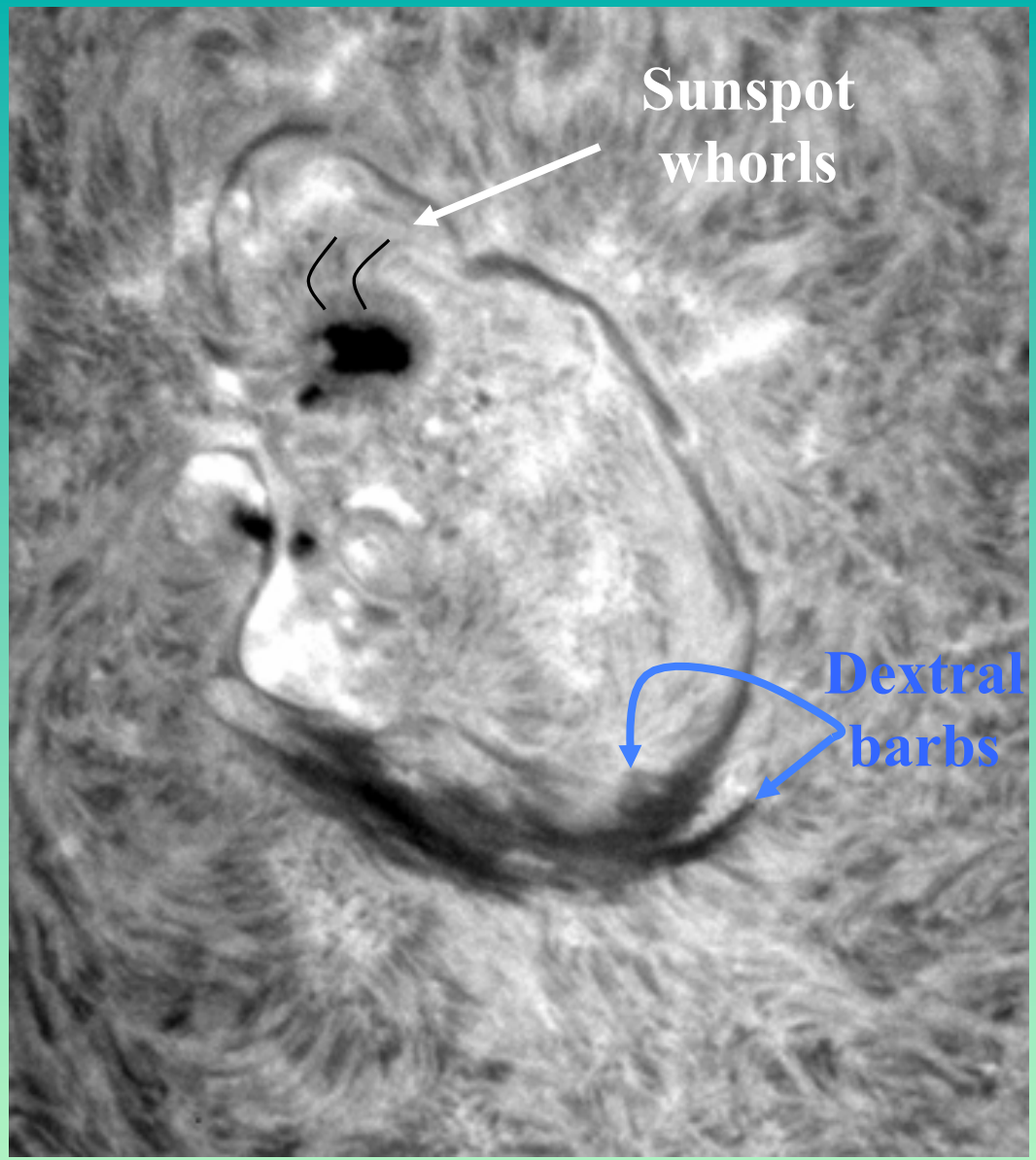

Sunspot whorls → $H_{AR} < 0$

Dextral barbs → $H_{AR} < 0$

ARIES image

Observational clues – Active region helicity sign

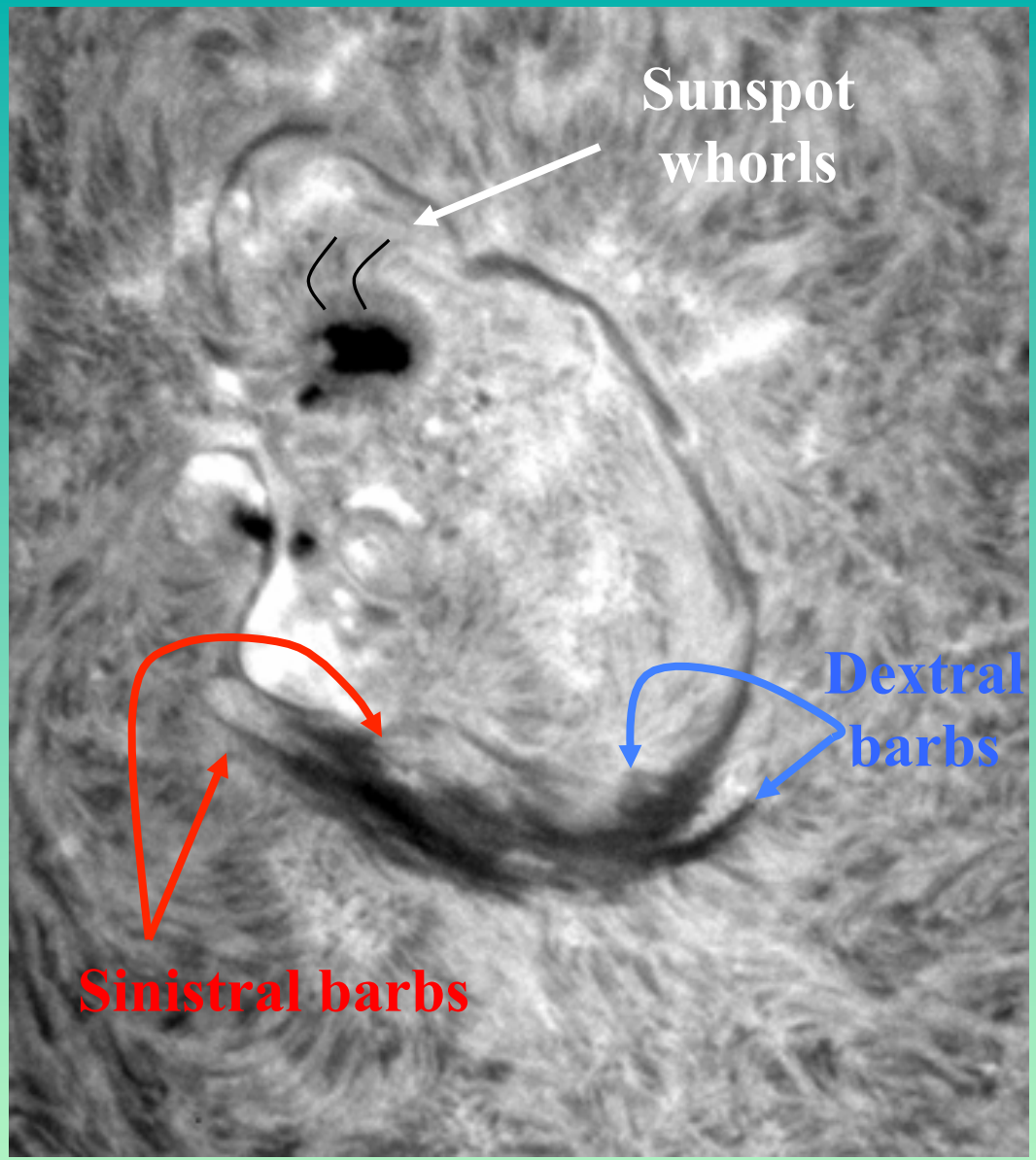

Sunspot whorls → $H_{AR} < 0$

Dextral barbs → $H_{AR} < 0$

Sinistral barbs → $H_{AR} > 0$

ARIES image

Origin of the first Magnetic cloud: Eruption of a filament and flare on 18 November 2003

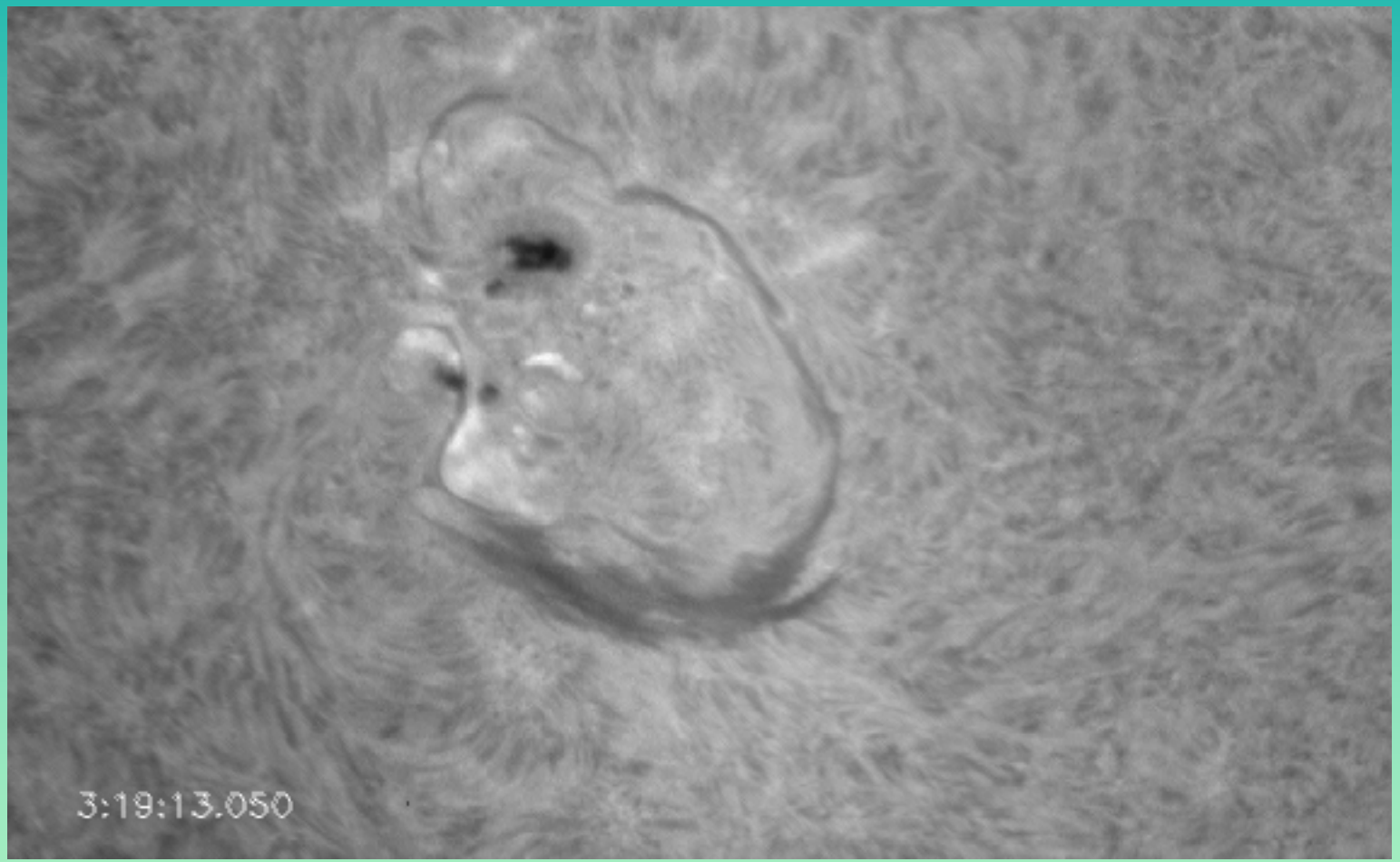

Nainital movie

Chandra et al. 2010

Post flare loops (TRACE)

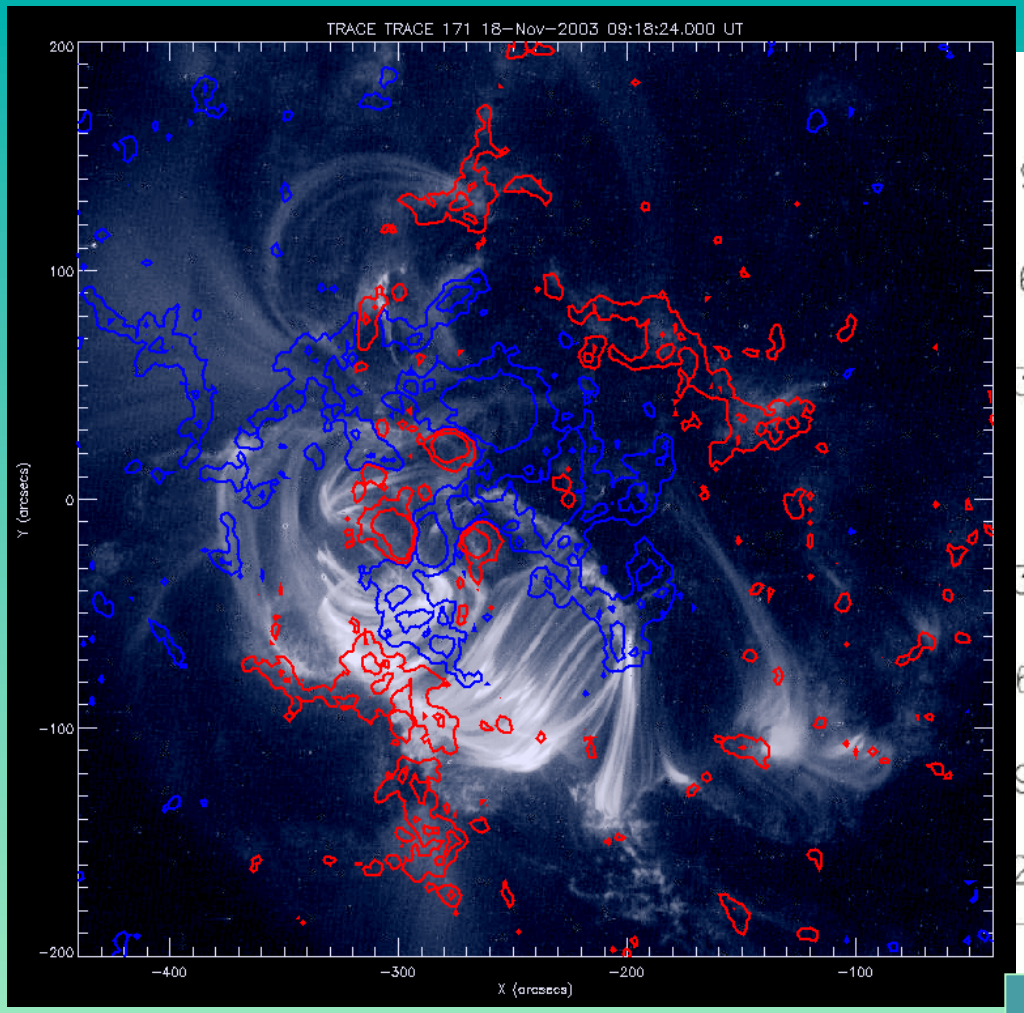

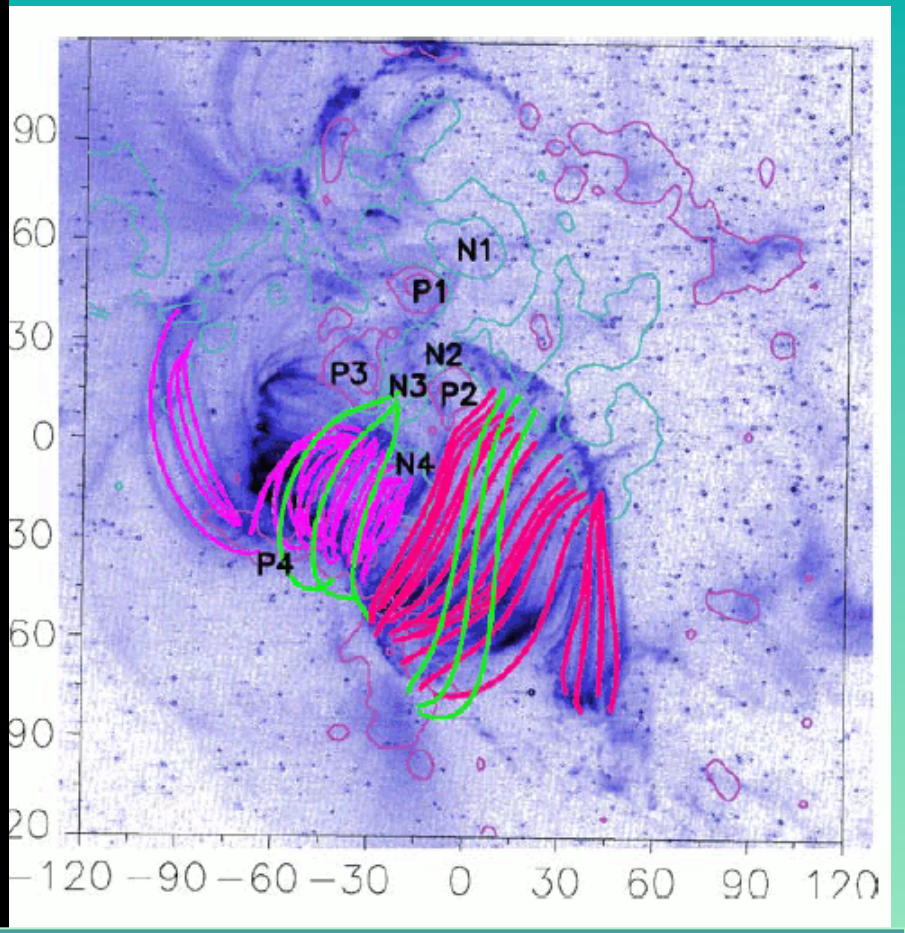

Extrapolation of field lines in the corona
Positive polarities (red) , negative (blue)

Chandra et al. 2010

H < 0

H > 0 → Positive magnetic helicity

H = 0

Progress in understanding the transient phenomena in the Sun-Earth system
Schmieder et al., 2011, Advances in Space Research, 47, 12, 2081

Exceptional cases understood (Events of 18 and 20 November 2003)

Magnetic clouds detected by ACE and Interplanetary coronal mass ejection (scintillation technique): Magnetic cloud have $H > 0$

BUT Active region have $H < 0$ (global negative magnetic helicity)

Conservation of the magnetic helicity in the Sun Earth system (Berger M. 1984) ?

Explanation

Emergence of new flux in the Active region to inject magnetic helicity that produces the large geo-effective event:

Complexity of the active region

Shearing and stress of the magnetic field

CME: kinetic energy of 3.3×10^{32} ergs with a a mass loss of 6×10^{13} kg

Magnetic helicity is conserved in Sun-Earth system due to launches of Coronal mass ejections

Prospective studies

Study of the three dimension topology of the magnetic field in the corona derived from vector magnetograms obtained in different lines.

Comparison of different vectors magnetograms obtained with different instruments.

Analyse of emerging flux observed in vector magnetograms (Hinode/SOT).

Data driven extrapolations.

Remote observations: Hinode, 17th may 2007

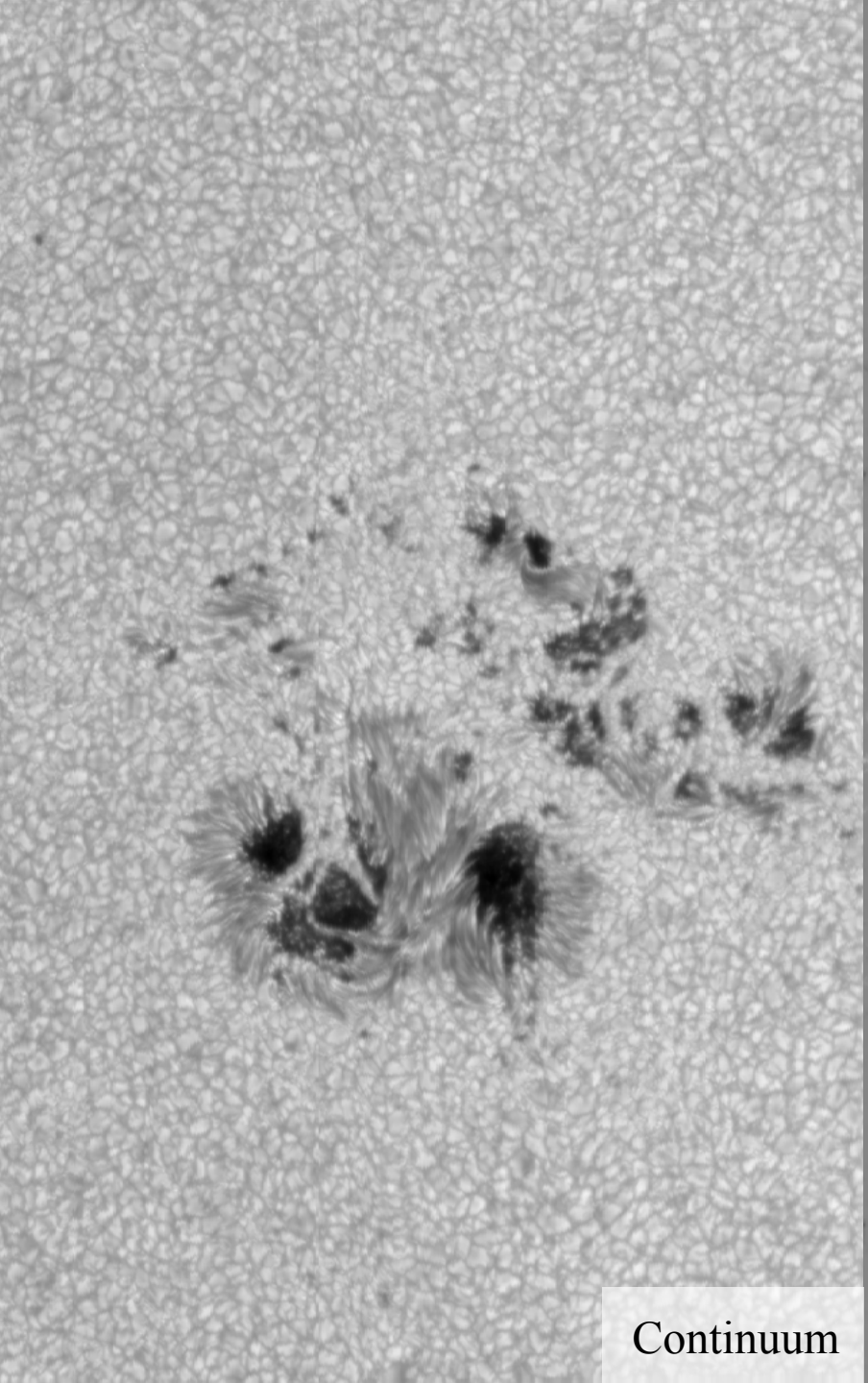

Continuum

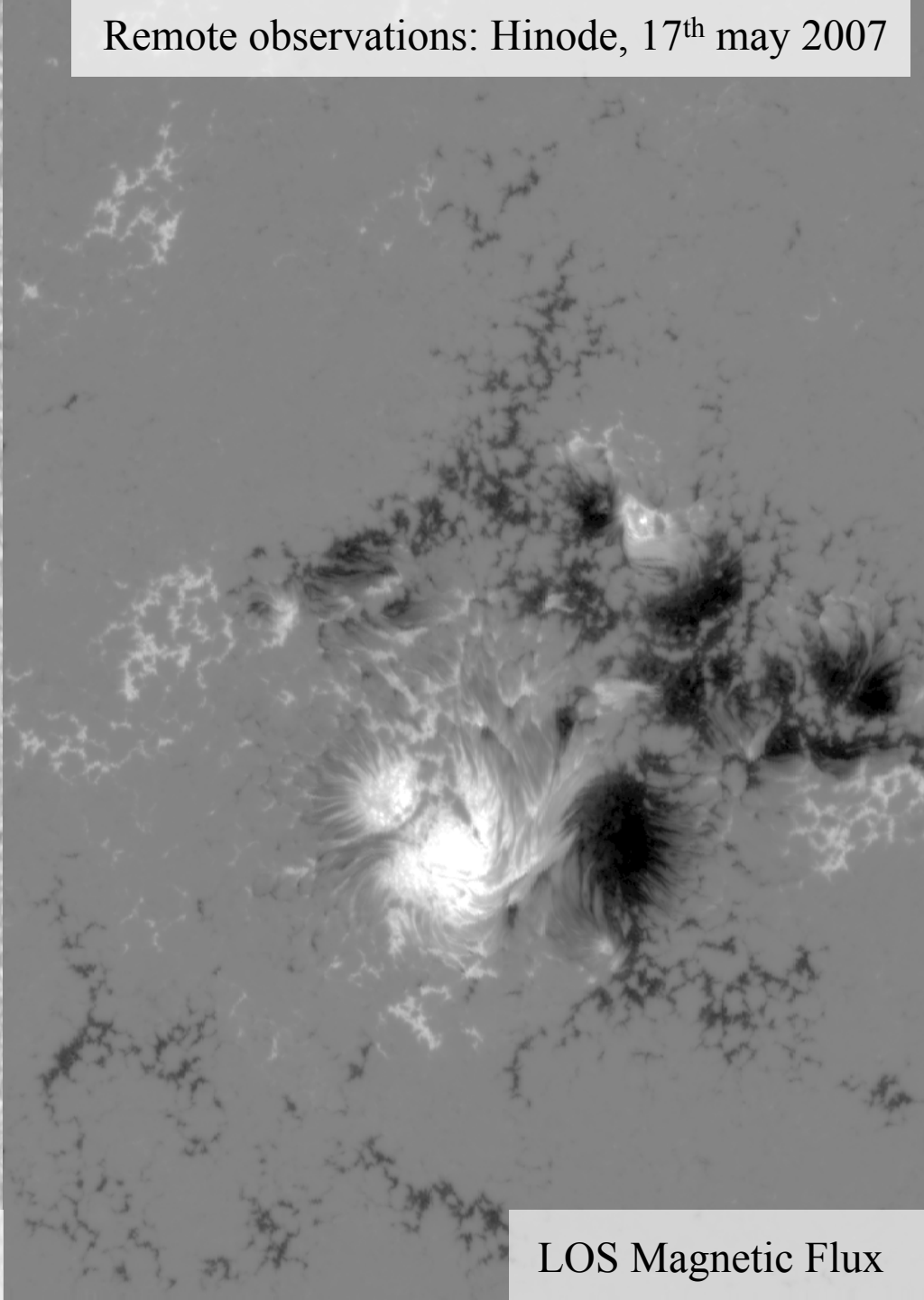

LOS Magnetic Flux

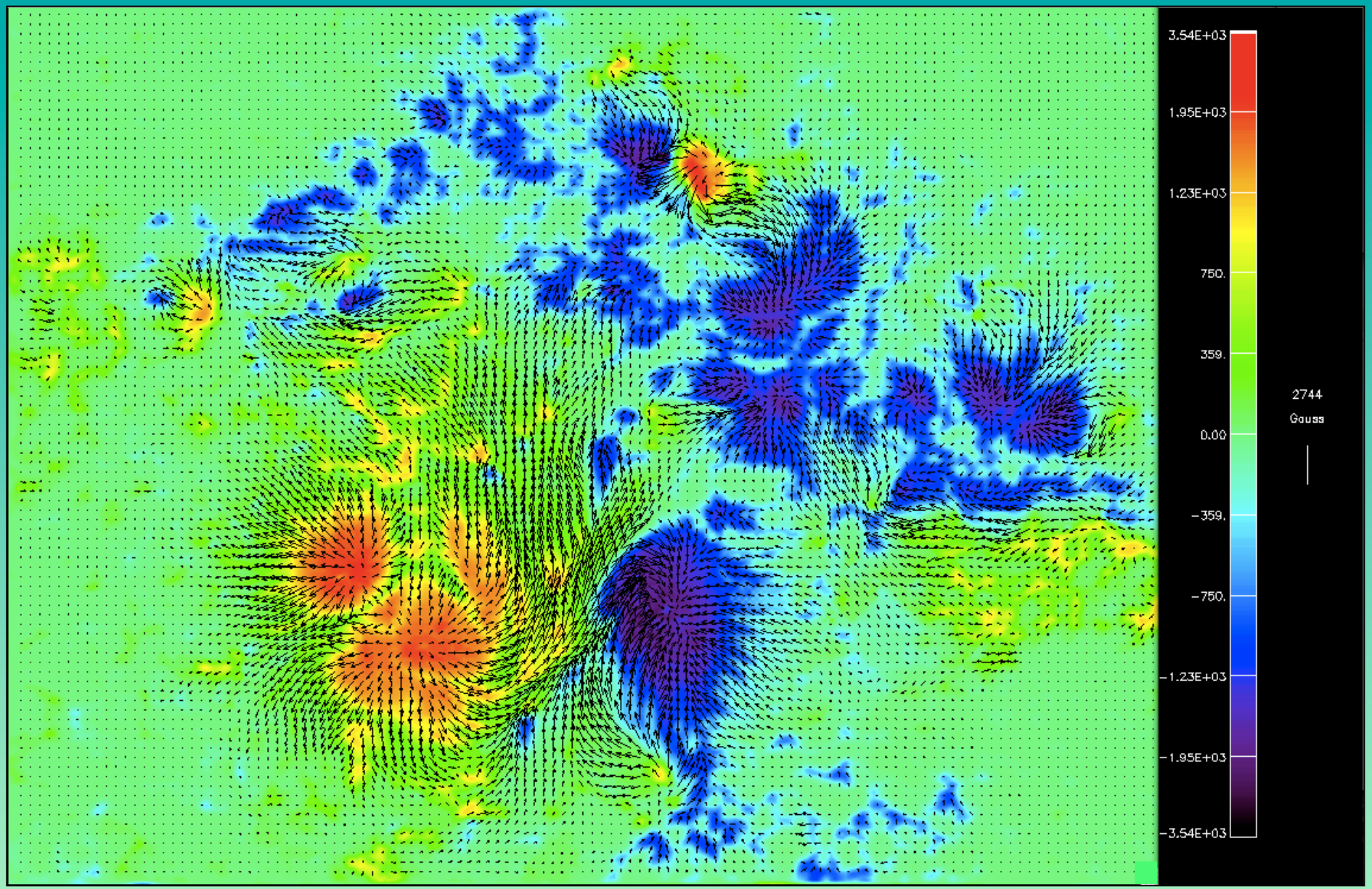

3D magnetic map 180° ambiguity resolved (Bommier et al., 2011)

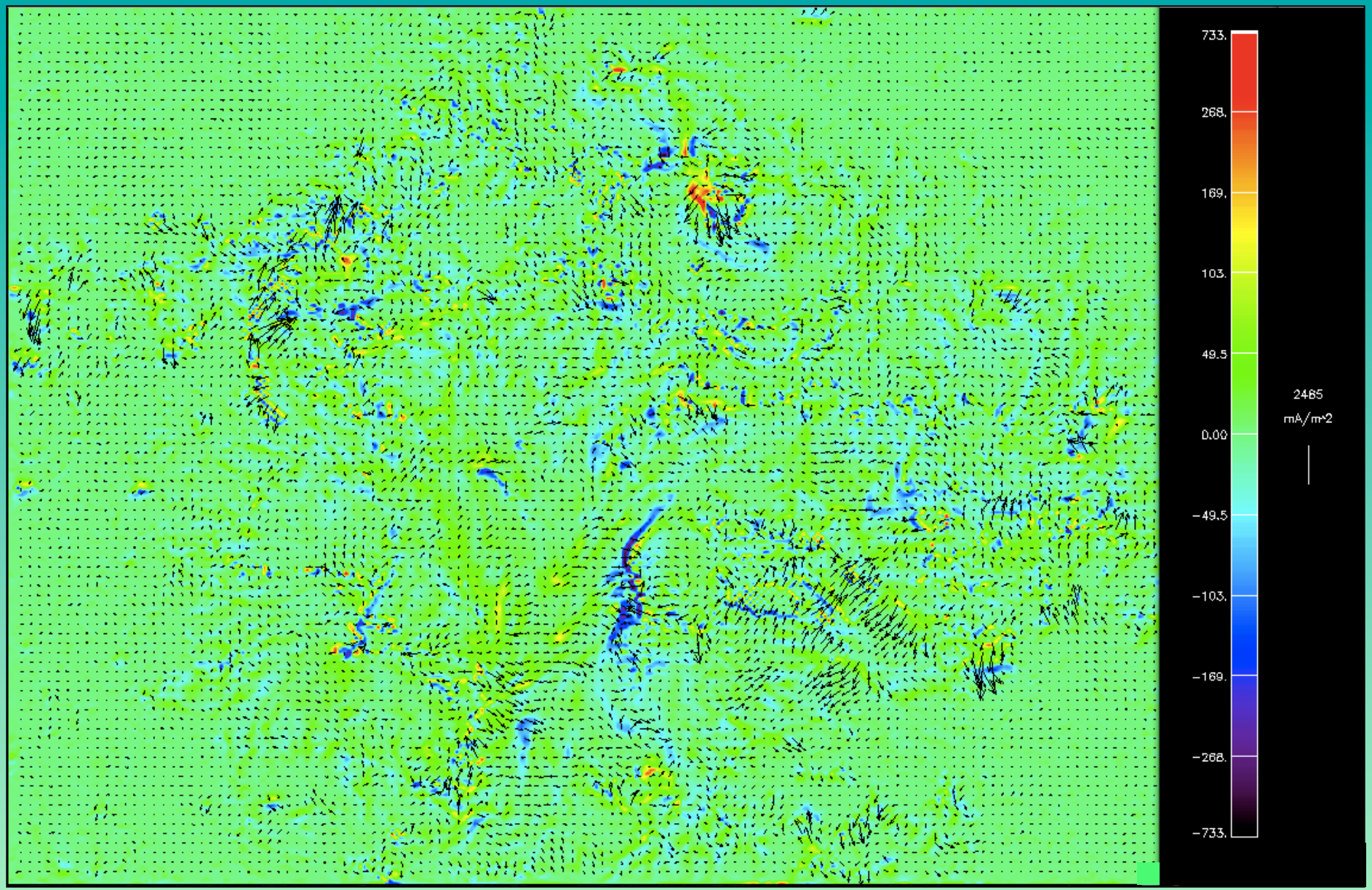

Current intensity

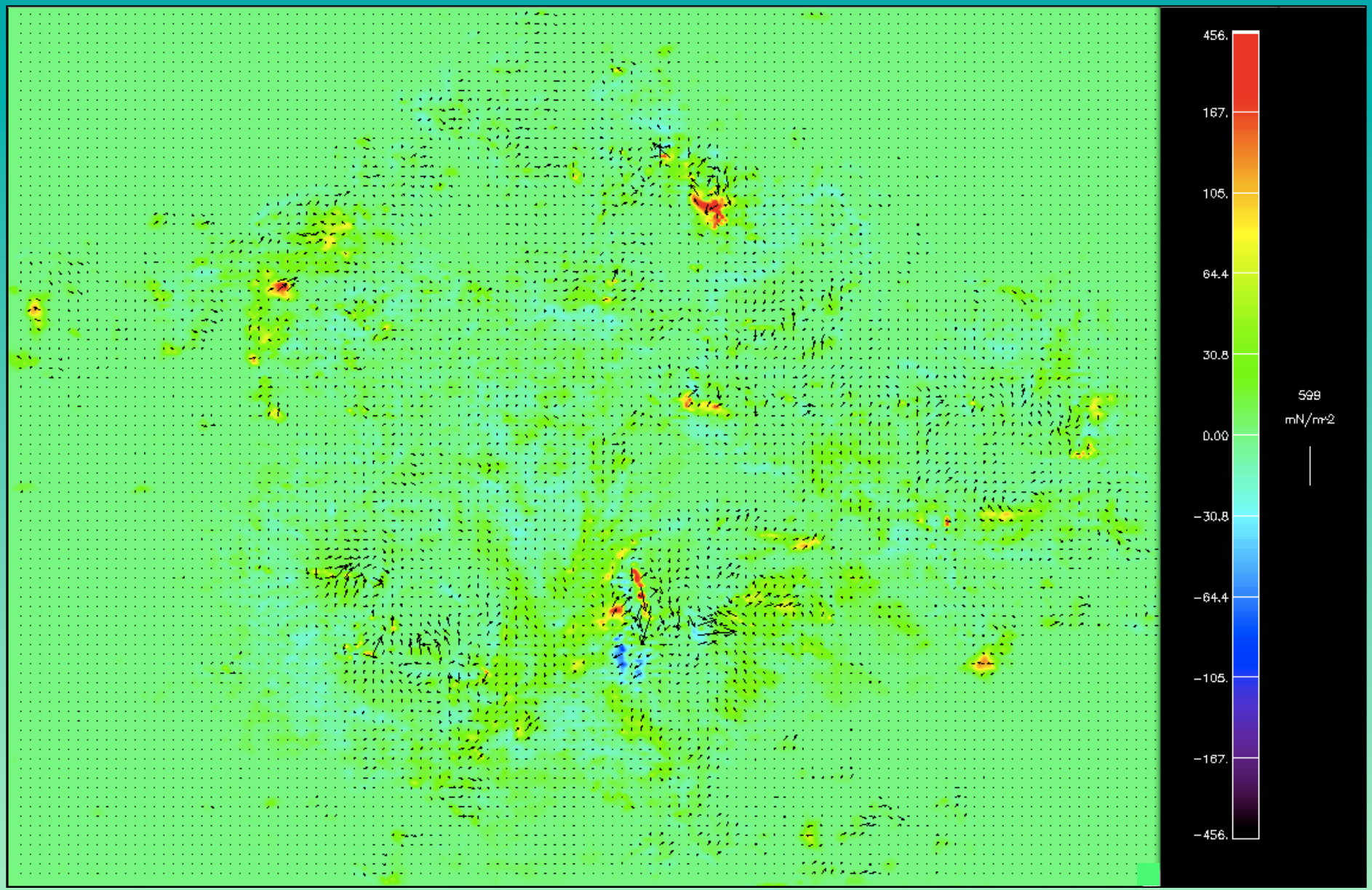

Lorentz force

THEMIS (ground based observations)

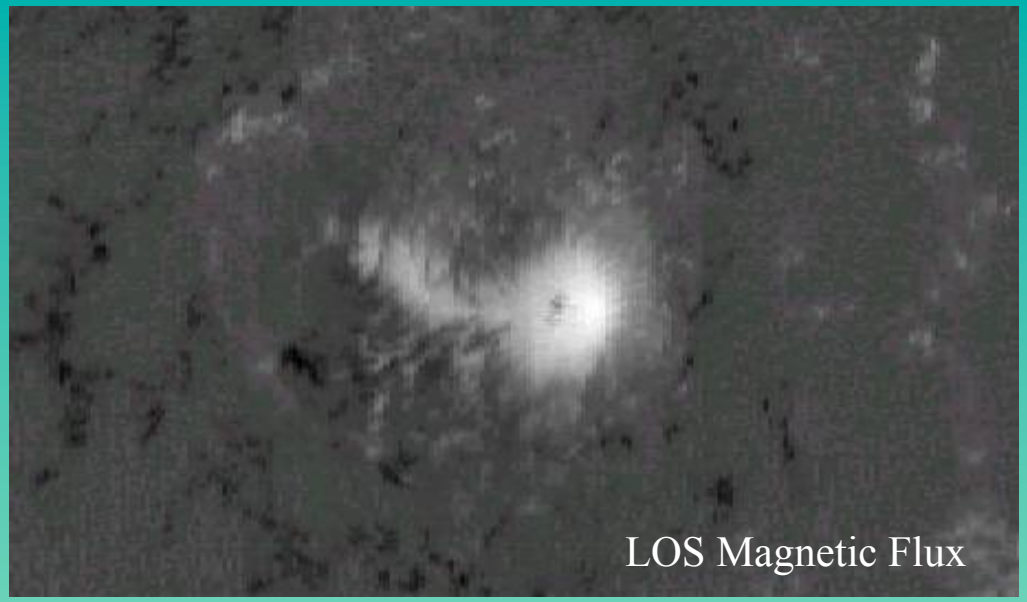

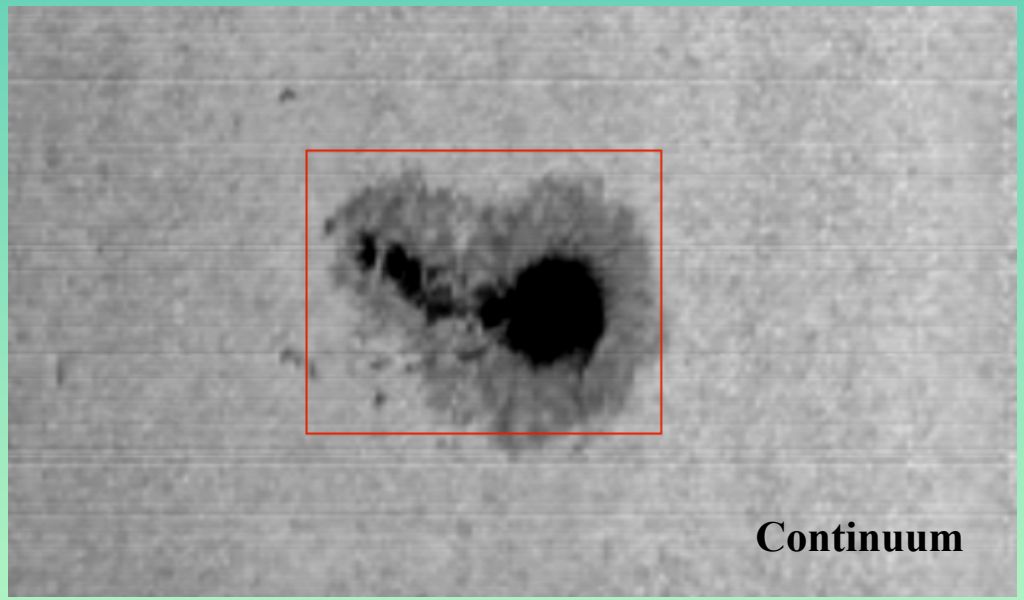

Hα BBSO

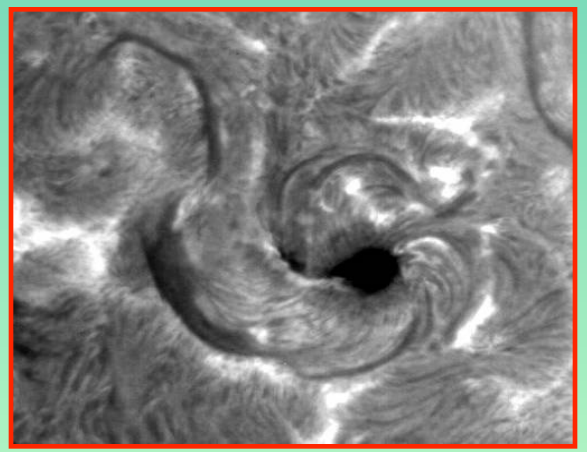

Ground multiline observations: THEMIS (up to 8 simultaneous lines)

(Molodij & Bommier, in prep.)

3D Magnetic Field

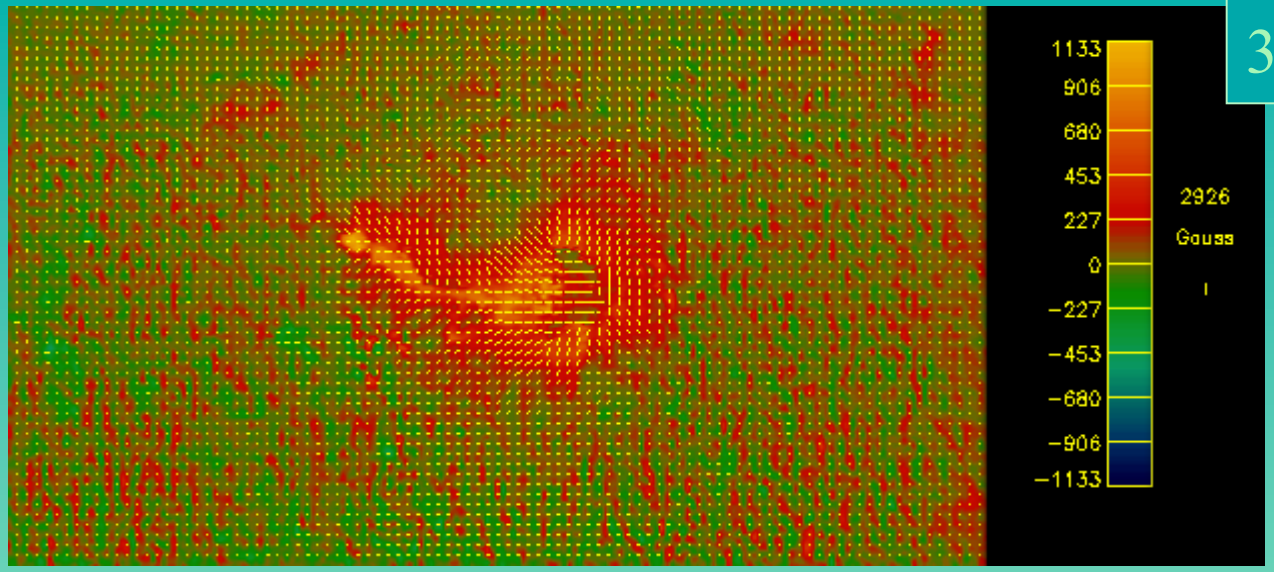

5250 A FeI

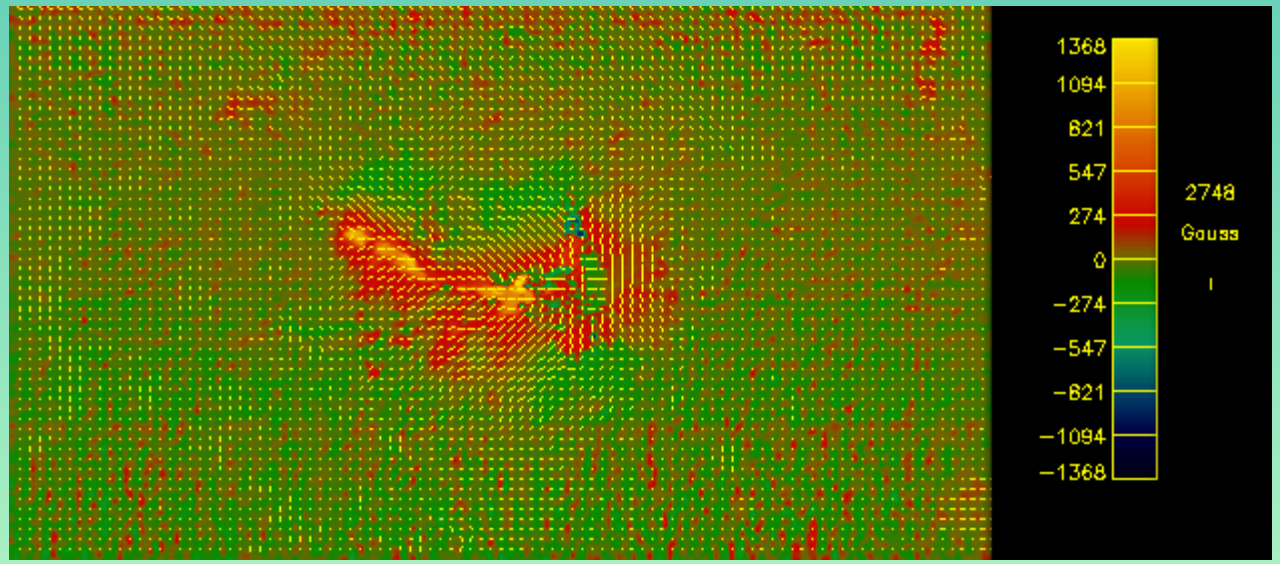

6302 A FeI

Horizontality

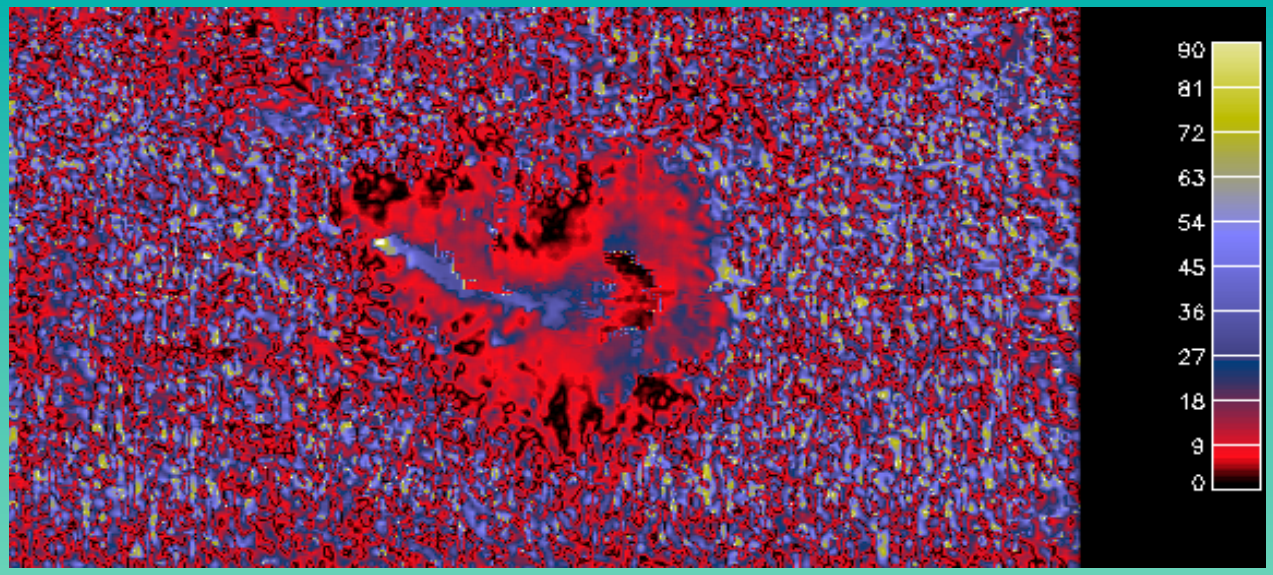

5250 A FeI

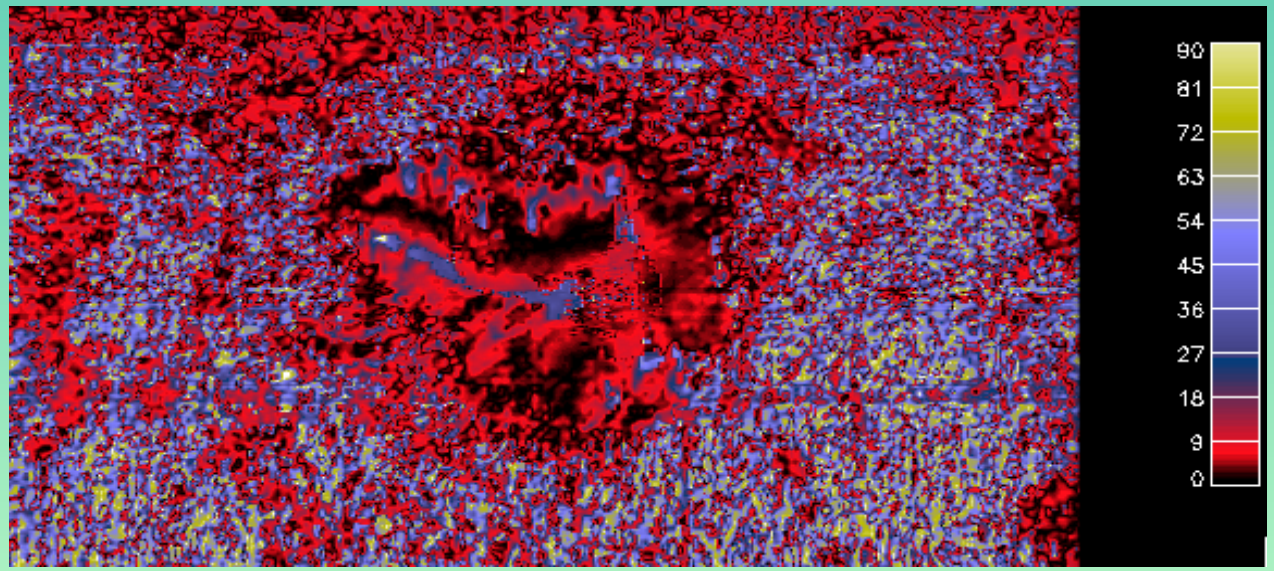

6302 A FeI

Inclination (LOS)

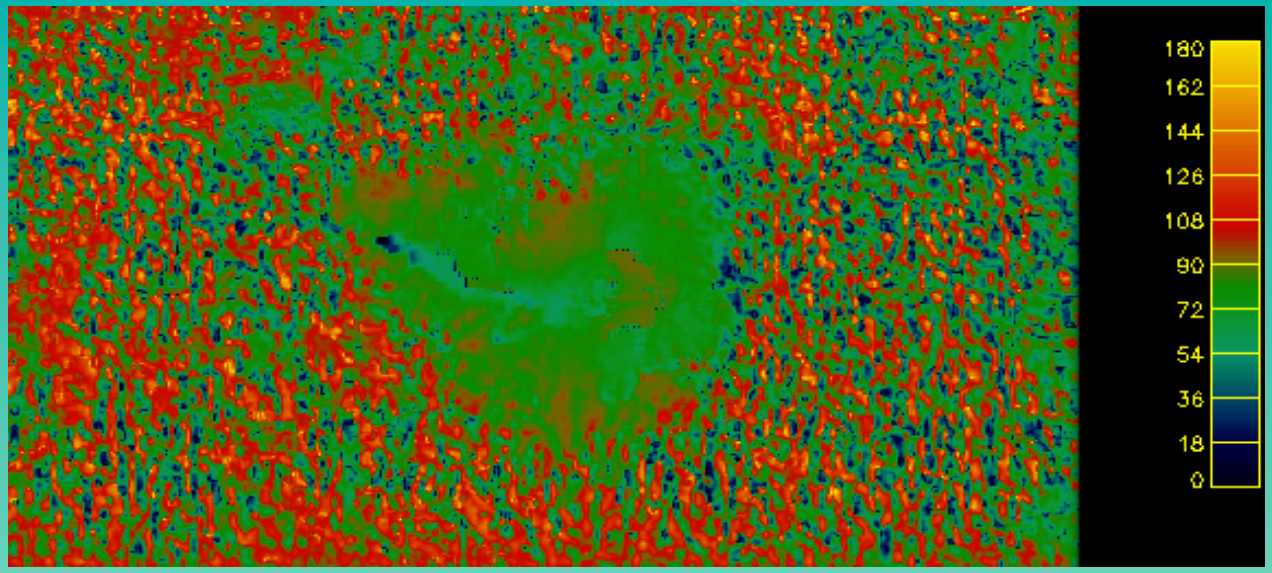

5250 A FeI

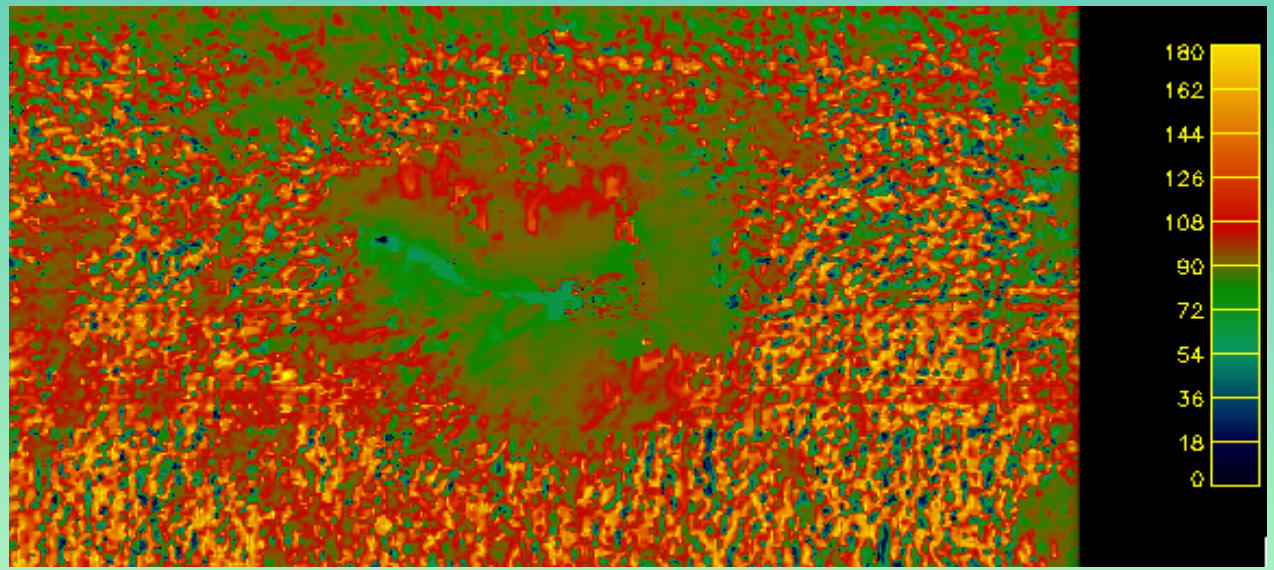

6302 A FeI

Magnetic Intensity

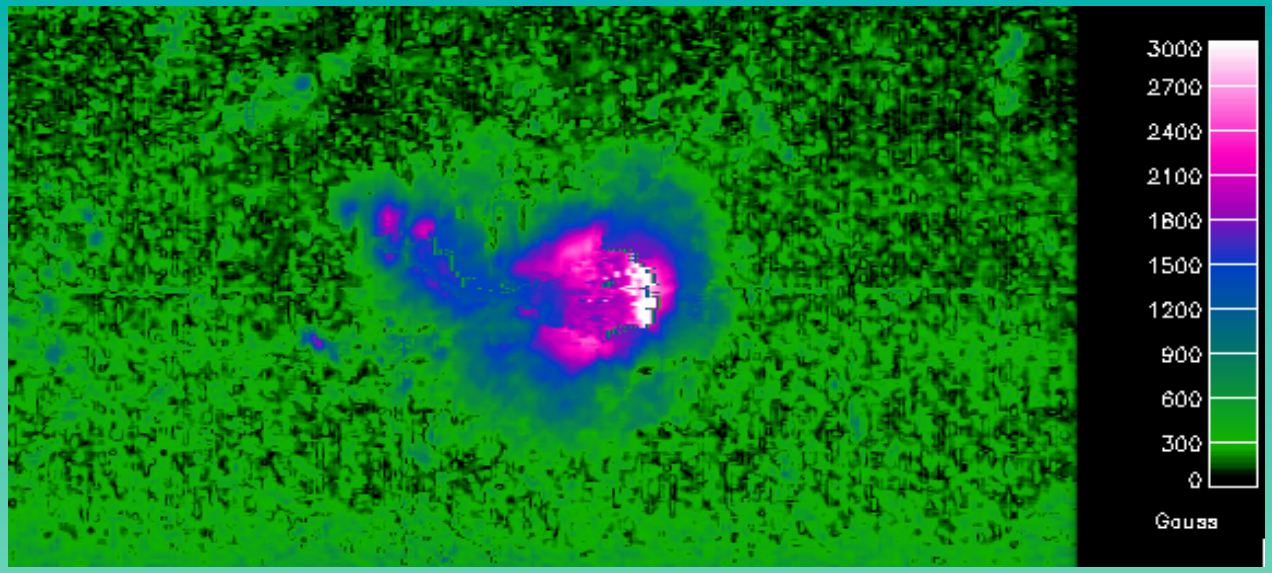

5250 A FeI

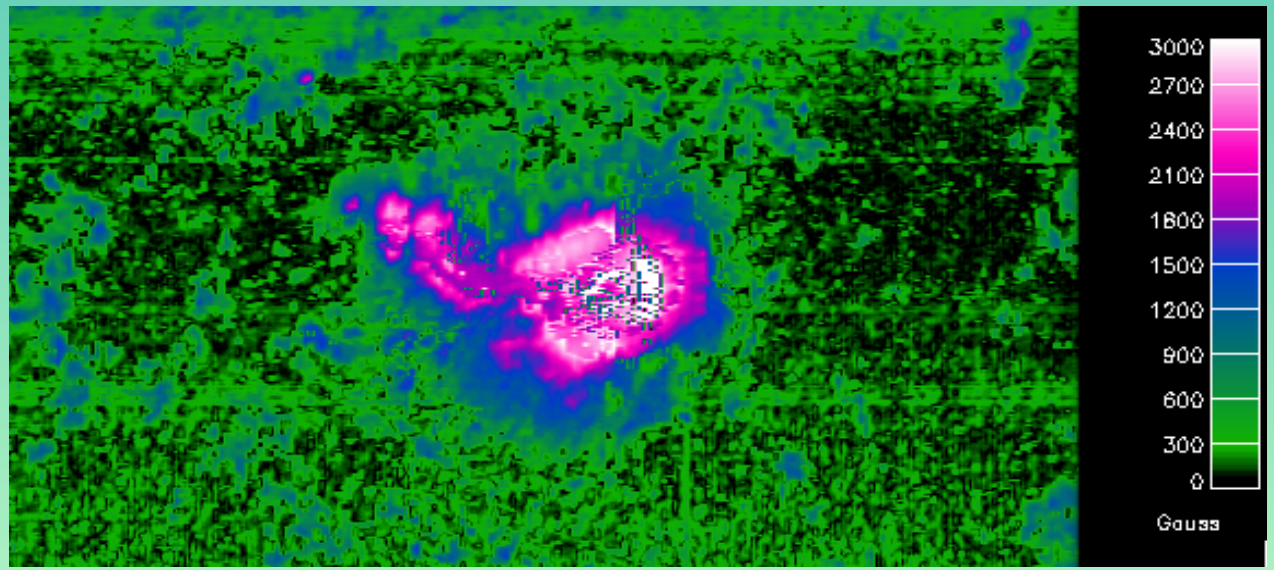

6302 A FeI

Inclusion of the velocity gradient in the Unno-Rachkovsky solutions

$$\begin{cases} \eta_p = \eta_0 \, \mathrm{e}^{-\left(\frac{\lambda-\lambda_0}{\xi}+\delta V_p\right)^2} \\ \eta_l = \eta_0 \, \mathrm{e}^{-\left(\frac{\lambda-\lambda_0}{\xi}-v_h+v_r+\delta V_l\right)^2} \\ \eta_r = \eta_0 \, \mathrm{e}^{-\left(\frac{\lambda-\lambda_0}{\xi}+v_h+v_r+\delta V_r\right)^2} \end{cases}$$

$$\begin{cases} \delta V_p = \dfrac{\delta_V}{\xi} \mathrm{e}^{-\left(\frac{\lambda-\lambda_0}{\xi}\right)^2} \\ \delta V_l = \dfrac{\delta_V}{\xi} \mathrm{e}^{-\left(\frac{\lambda-\lambda_0}{\xi}-v_h+v_r\right)^2} \\ \delta V_r = \dfrac{\delta_V}{\xi} \mathrm{e}^{-\left(\frac{\lambda-\lambda_0}{\xi}+v_h+v_r\right)^2} \end{cases}$$

$$\begin{cases} v_r = \alpha \dfrac{v_s}{\xi} \\ v_h = \dfrac{4.67.10^{-2} \lambda^2 \bar{g} H}{\xi} \end{cases}$$

radial velocity

Zeeman shift

α constant to convert velocity in Doppler width unity

v_s velocity (m/s)

ξ Doppler width

η_0 absorption coefficient at the line center

$\bar{g}$ effective Landé factor

H magnetic field strength

Velocity gradients

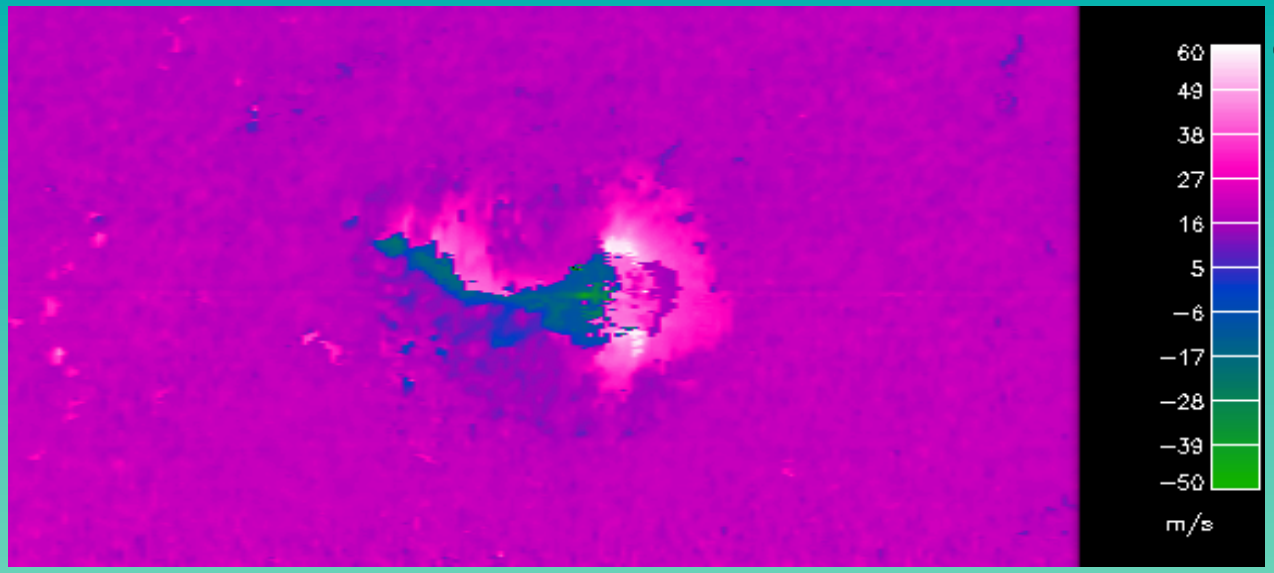

5250 A FeI

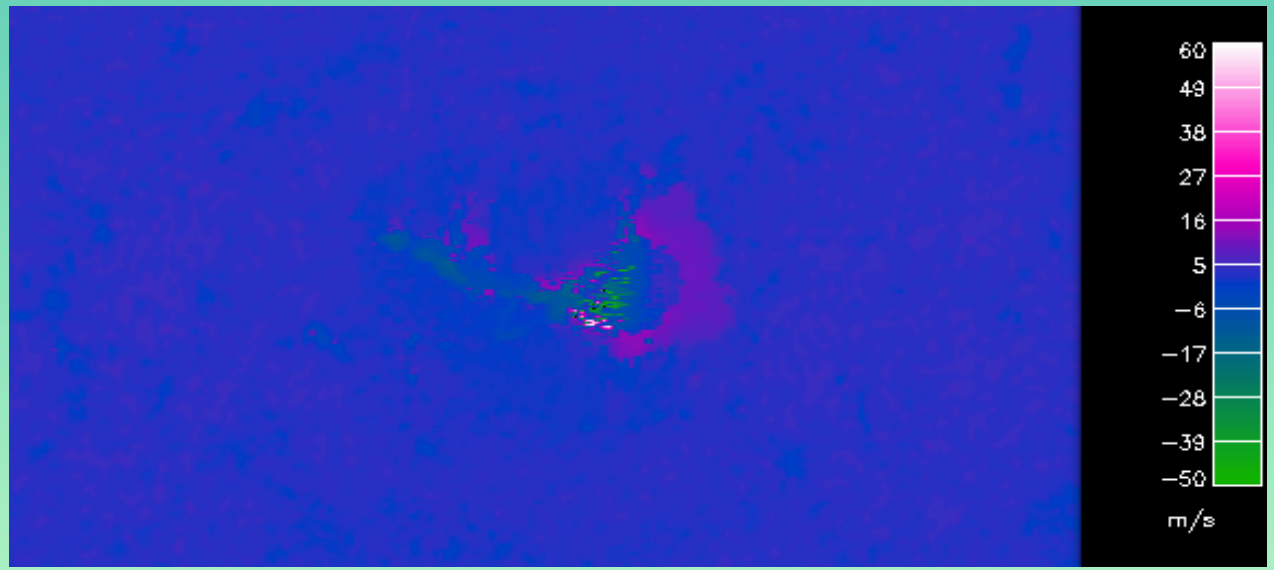

6302 A FeI

Molodij et al., 2011

Conclusion

Progress in understanding the transient phenomena in the Sun-Earth system
Schmieder et al., 2011, Advances in Space Research, 47, 12, 2081

Precise identification of the solar source of coronal mass ejections linked to flares, filaments eruptions and to interplanetary magnetic clouds. Most strong geo-effective case of solar cycle 23 (Chandra et al.,2010, Schmieder et al., 2011). Flare ribbons are identified (Chandra et al. 2009).

The computation of the magnetic helicity could be treated routinely to forecast the disturbances of large magnetic clouds. (Srivastava et al 2009, Chandra et al 2010, 2011, Kumar et al 2010, Torok et al 2011)

A combination of vector magnetograms and Hα observations is of great interest for the forecast of ejections of coronal mass in the interplanetary medium (Gosain et al 2009, 2010, Artzner et al 2010)